

The effects of opposite-polarity dipoles on the detection of Glass patterns

David Burr^{a,b,*}, John Ross^c

^a *Istituto di Neuroscienze del CNR, Pisa 56100, Italy*

^b *Dipartimento di Psicologia, Università di Firenze, Italy*

^c *School of Psychology, The University of Western Australia, Perth WA, Australia*

Received 23 May 2005; received in revised form 6 September 2005

Abstract

Glass patterns—randomly positioned coherently orientated dipoles—create a strong sensation of oriented spatial structure. On the other hand, coherently oriented dipoles comprising dots of opposite polarity (“anti-Glass” patterns) have no distinct spatial structure and are very hard to distinguish from random noise. Although anti-Glass patterns have no obvious spatial structure themselves, their presence can destroy the structure created by Glass patterns. We measured the strength of this effect for both static and dynamic Glass patterns, and showed that anti-Glass patterns can raise thresholds for Glass patterns by a factor of 2–4, increasing with density. The dependence on density suggests that the interactions occur at a local level. When the Glass and anti-Glass dipoles were confined to alternate strips (in translational and circular Glass patterns), the detrimental effect occurred for stripe widths less than about 1.5°, but had little effect for larger stripe widths, reinforcing the suggestion that the interaction occurred over a limited spatial extent. The extent of spatial interaction was much less than that for spatial summation of these patterns, at least 30° under matched experimental conditions. The results suggest two stages of analysis for Glass patterns, an early stage of limited spatial extent where orientation is extracted, and a later stage that sums these orientation signals.

© 2005 Elsevier Ltd. All rights reserved.

Keywords: Spatial vision; Psychophysics; Glass patterns; Form analysis

1. Introduction

Glass patterns, composed of randomly positioned dipoles that are coherently oriented, carry a powerful sense of global spatial structure when the elements within a dipole are of the same contrast (Glass, 1969; Glass & Perez, 1973). When the coherently oriented dipoles comprise dots of opposite polarity (“anti-Glass” patterns), there is a lack of distinct global structure that is hard to distinguish from random noise (Badcock, Clifford, & Khuu, 2005; Glass & Switkes, 1976; Prazdny, 1986). Kovacs and Julesz (1992) report that, under conditions of polarity reversal, subjects tended to make orthogonal errors, reporting horizontal

patterns as vertical (and vice versa) and circular patterns as radial (and vice versa). Wilson, Switkes, and De Valois (2004) do not report any tendency to make orthogonal errors, finding instead that large contrast differences within dipoles totally abolish the perception of global pattern.

From an analysis of their Fourier spectra, Barlow and Olshausen (2004) concluded that anti-Glass patterns, despite their innocuous appearance, should have a potent effect when added to Glass patterns. They report an absence of the appearance of global structure when Glass and anti-Glass patterns are mixed at equal strength. Our purpose in this study was to quantify the destructive effects of anti-Glass patterns reported by Barlow and Olshausen and to try to understand the mechanisms at work. In particular, we were interested whether the effects were global, as implied by considerations of the power spectra, or local.

* Corresponding author. Tel.: +39 348 3972198.
E-mail address: dave@in.cnr.it (D. Burr).

Fig. 1 shows examples of the patterns we used. Figs. 1A and B show a section of a translational Glass pattern, together with its Fourier amplitude spectrum. The pattern

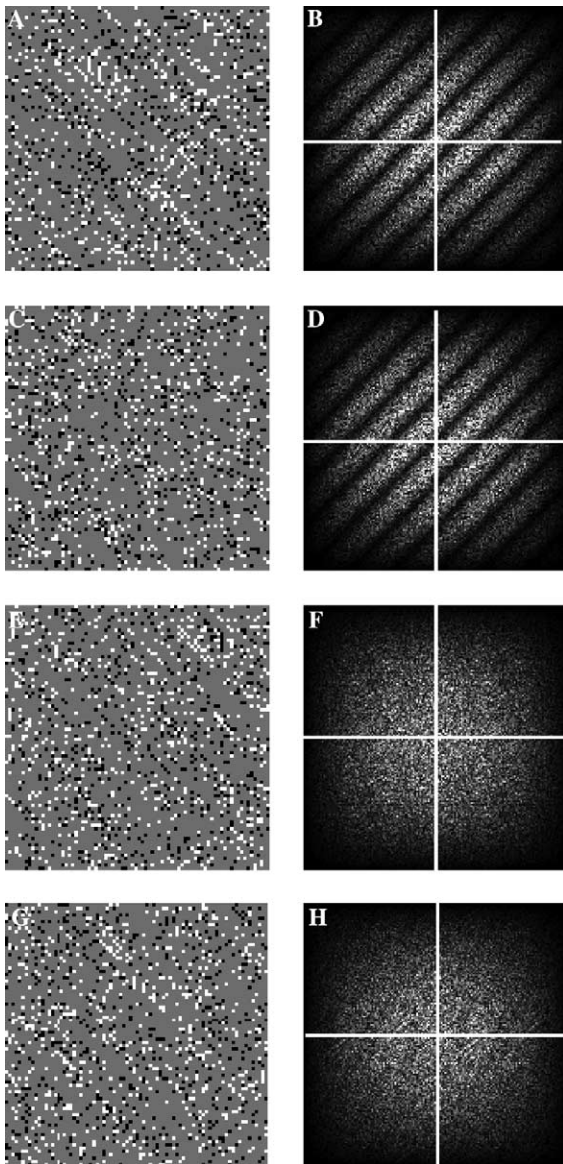


Fig. 1. Examples of the patterns used in this study. (A) A section of a translational Glass pattern (about 1/3 of the width of the actual pattern). The pattern has oriented structure at -45° . (B) Fourier amplitude spectrum of (A). The modulation is cosinusoidal, oriented at $+45^\circ$. (C) An “anti-Glass” pattern, where the pairs all have opposite contrast. The pattern has no clear orientation. (D) Amplitude spectrum of (C). The modulation is sinusoidal, oriented at $+45^\circ$. There is no clear bias of energy along a particular orientation, but rather an absence of energy along the $+45^\circ$ diagonal. (E) The sum of a Glass and anti-Glass pattern. There is little or no impression of oriented structure, showing that although the anti-Glass pattern has no clear structure itself, it can destroy that of the Glass pattern. (F) Amplitude spectrum of (E). There is no anisotropy, as this spectrum is derived from the sum of the squared cosinusoidal spectrum of the Glass pattern and the squared sinusoidal modulation of the anti-Glass pattern. (G) Glass and anti-Glass stimuli confined to alternating stripes 2° wide (when viewed from the correct distance). The striped structure can be seen in this stimulus. (H) Amplitude spectrum of (G). This is virtually indistinguishable from (F), as the global power is not affected by dividing the Glass from anti-Glass patterns.

has a clearly oriented structure at -45° , reflected in the orientation bias at $+45^\circ$ of its amplitude spectrum. Figs. 1C and D show an anti-Glass pattern with amplitude spectrum. The pattern has no clear orientation, and this is reflected in the lack of any clear bias of energy along a particular orientation, but rather an absence of energy along the diagonal. Fig. 1E shows the sum of a Glass and anti-Glass pattern. There is little or no impression of oriented structure, showing that although the anti-Glass pattern has no clear structure itself, it can destroy that of the Glass pattern. This is reflected in its amplitude spectrum (Fig. 1F), that shows no anisotropy (being the sum of the squared cosinusoidal spectrum of the Glass pattern and the squared sinusoidal modulation of the anti-Glass pattern). Fig. 1G shows Glass and anti-Glass stimuli confined to alternating stripes 2° wide (when viewed from the correct distance). The striped structure can be seen in this stimulus. Fig. 1H shows that curtailment into stripes does not affect the global Fourier power spectrum.

2. Methods

The stimuli were computed within Matlab and displayed on the face of a Hitachi (HM-4821-D) monitor via a Visage Framestore (Cambridge Research Systems) at a resolution of 640×480 pixels and 170 Hz. The screen (mean luminance 32 cd/m^2) was $35 \times 27 \text{ cm}$, subtending $32 \times 25^\circ$ at the viewing distance of 60 cm. All patterns were comprised of dots, 2×2 pixels (0.1°) half white and half black.

The target stimuli for all studies were “Glass patterns”, formed by pairs of like-coloured dots oriented in a coherent manner. Patterns were either translational, with all pairs oriented at -45° , or circular, with pairs oriented tangentially. The separation of the pairs was always 0.4° . The “anti-Glass” patterns were identical to the Glass patterns, except the two dots were of opposite sign (randomly black-white or white-black). Fig. 1 shows examples of the patterns used in this study. Glass patterns were either standard static patterns, or “dynamic” patterns, updated every 16 video-frames (10.6 Hz) with fresh random Glass patterns and anti-Glass patterns. These dynamic Glass patterns give an impression of motion along the direction of the dot orientation, although there is no excess of spatio-temporal energy in that direction (Ross, Badcock, & Hayes, 2000). All presentations, both static and dynamic, were 1 s in duration, vignettted within a Gaussian window of $\sigma = 250 \text{ ms}$.

Thresholds were measured by a two-interval forced-choice procedure, where the subject was required to identify which interval contained the Glass pattern (the anti-Glass patterns were identical in the two presentations). Signal-to-noise ratios were varied by the adaptive routine QUEST (Watson & Pelli, 1983) to home in near threshold. Thresholds were calculated by fitting a cumulative Gaussian. Standard errors were estimated by 500 repetitions the bootstrap technique (Efron & Tibshirani, 1993).

Two type of noise were used: randomly positioned randomly oriented dipoles of matched separation (for the density measurements); or noise dots that were completely uncorrelated spatially (for the interaction and summation measurements). The reason for varying the procedure from the more standard randomly oriented pairs was that when confined to narrow stripes parallel to dipole orientation, randomly oriented pairs would spill over the confines. In practice, both techniques had similar effects on threshold, as can be verified by comparing appropriate points of Figs. 2 and 4.

In the first experiment (effect of density) the Glass and anti-Glass patterns were presented on alternative frames (at 170 Hz): the physical contrast was always 1, but the effective contrast (taking temporal integration into account) was 0.5. The proportion of correlated pairs (either Glass or anti-Glass) to randomly oriented pairs was always the same, both varying together with signal-to-noise level. No attempt was made to avoid overlap of dots, so at high densities, both the actual density and the signal-to-noise ratio were less than the theoretical measures. Actual density (the percentage of pixels differing from mean-luminance) was therefore measured in all conditions, as was the signal-to-noise ratio (by cross correlation), and these values are reported in the figures. In practice the difference became appreciable only for densities greater than 30%.

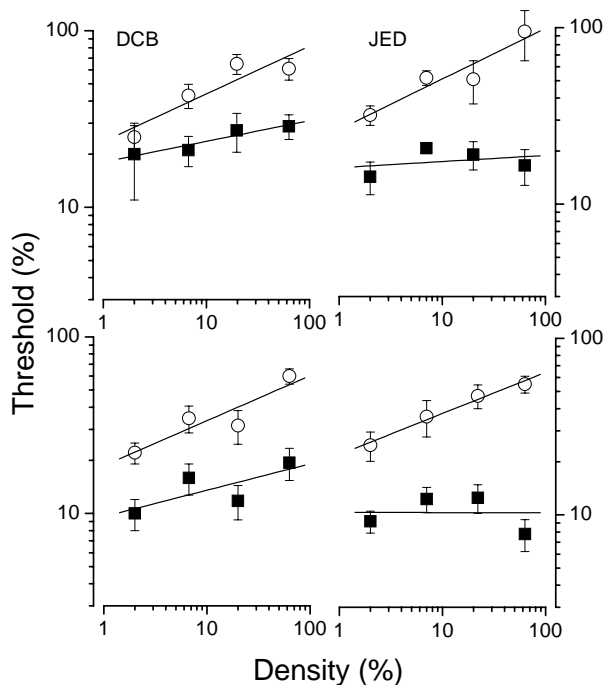


Fig. 2. Thresholds for detecting the interval containing the Glass pattern in a two-interval forced choice paradigm, as a function of density. The upper curves show results for static stimuli, lower curves for randomly changing stimuli (10.6 Hz). Open circles refer to thresholds measured in the presence of anti-Glass patterns, filled squares to the control condition where the anti-Glass patterns were substituted with uncorrelated noise of matched density. The straight lines show best-fitting linear regressions (on log–log coordinates).

For the measurement of the spatial extent of interaction, the Glass and anti-Glass patterns were confined to stripes of variable width, parallel to the orientation of the Glass patterns (-45° stripes for the translational pattern, annuli for the circular pattern). In this case the contrast was 0.5 and the density was always 22%. For the control stimuli, the anti-Glass patterns were replaced with uncorrelated noise of the same density. For each experimental condition (density, stripe width, etc.), thresholds were measured both for the anti-Glass and control conditions, intermingled within a single session (50 trials in total). Five sessions were run for each condition, randomising conditions between sessions.

In the final experiment measuring spatial summation of Glass patterns, the Glass stimuli were confined to a central area, diamond shaped for the translational pattern, circular for the circular pattern. The width or diameter was varied. No anti-Glass pairs were used for this study.

Complete measurements were made for two observers, one author and one trained subject naïve to the goals of the experiment. All major effects were verified more informally by the other author.

3. Results

3.1. Effect of density

The first experiment was designed to quantify the magnitude of the effect reported by Barlow and Olshausen (2004), and test whether it depends on pattern density. Subjects were asked to discriminate the interval containing the Glass pattern from one containing randomly oriented dipoles in two conditions: when the patterns were superimposed on an anti-Glass pattern of matched density, or on randomly oriented dipoles of matched density. The results for two observers are shown in Fig. 2. For all densities, for both static and dynamic Glass patterns, thresholds were higher when the Glass patterns were superimposed on anti-Glass patterns (open circles) than on randomly oriented dipoles in (filled squares). The effect was greater at high than at low densities, ranging from a factor of 2 at 2% density to 4.5 at 65% density. The dashed lines are best linear fits of the data (on logarithmic coordinates), giving average log–log slopes of 0.26 (near fourth-root relationship). The higher the density, the greater the effects of the anti-Glass patterns, suggesting that the interactions occur over a limited range, so are more effective at high densities. For the control measurements, sensitivity was roughly constant with density at about 10% (equivalent to 5% in standard conditions, given the extra noise pedestal), with average log–log slope of 0.07, consistent with previous reports (Dakin, 1997; Wilson & Wilkinson, 1998). Fig. 3 shows the slopes of the density relationship as a bar graph.

3.2. Spatial range of interaction

The dependency on density suggests that the detrimental effects of anti-Glass patterns occur over a limited range. To test this notion more directly, we created stimuli with the

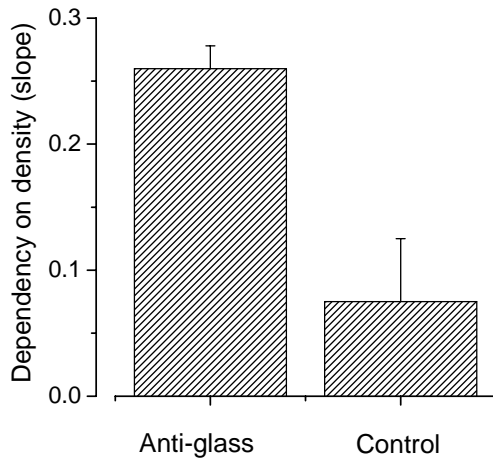


Fig. 3. Dependency of Glass thresholds on pattern density. The bars show the average slope of the regression lines of Fig. 2 (averaged over static and dynamic for both subjects), together with the standard errors. The dependency with anti-Glass patterns is 0.26, implying a fourth-root relationship, whereas the dependency in the control condition is only 0.07.

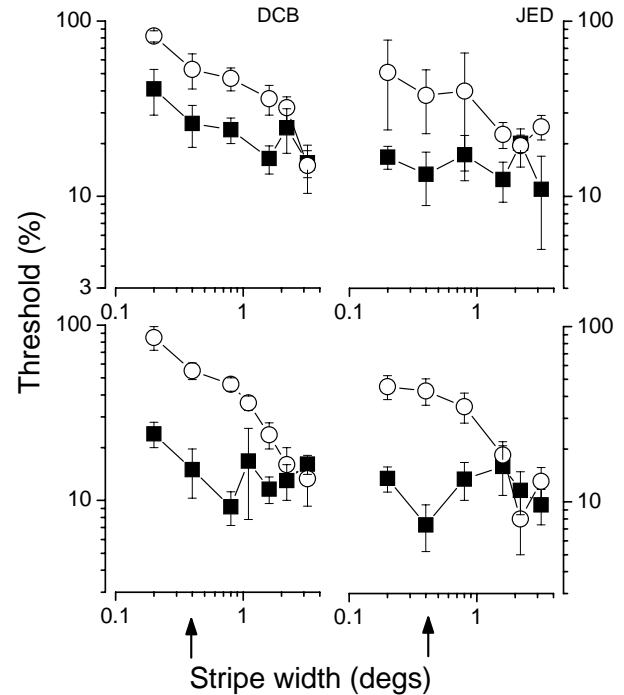


Fig. 5. Same as Fig. 4, except for circular rather than translational Glass patterns.

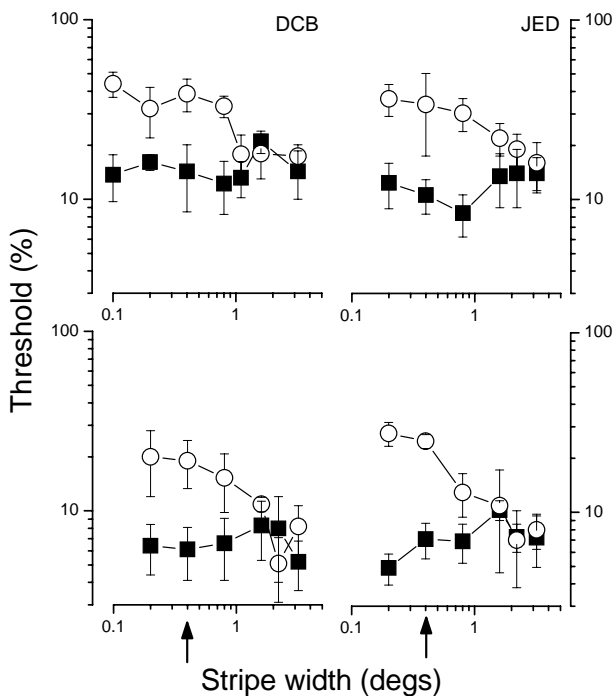


Fig. 4. Effect of confining Glass and anti-Glass stimuli to stripes parallel to the direction of dipole orientation, for various stripe widths. The arrows indicate the separation of the Glass and anti-Glass dipoles. Following the conventions of Fig. 2, upper curves show results for static stimuli, lower curves for randomly changing stimuli (10.6 Hz), open circles thresholds measured with anti-Glass patterns, filled squares to the control condition of uncorrelated noise of matched density. For narrow stripe widths, the thresholds with anti-Glass patterns were higher than the controls, by a factor of about 3, but the curves converge for widths of about 1.6°. This implies that the interference occurs over a limited range.

Glass and anti-Glass couples confined to alternate stripes parallel to the orientation of the dipoles (see Fig. 1H). In this case, the noise dots were not randomly oriented dipoles (that would over-spill the confines) but pairs of dots indi-

vidually positioned at random. The exact position of the stripes was randomised from trial to trial, and their width varied between sessions.

The results for diagonal Glass patterns are shown in Fig. 4. The pattern of results was similar for both static (upper curves) and dynamic (lower curves) Glass patterns. For narrow stripe-widths, thresholds were higher for the anti-Glass condition than for the noise control, by about a factor of about three, as before. However, for stripe separations greater than 1.6° (four times dipole separation), the two curves converge, with very little difference between the anti-Glass and the noise-control conditions.

Fig. 5 shows similar results for circular Glass patterns, with the Glass and anti-Glass dipoles confined to alternate annuli. The pattern of results is very similar to that for diagonal Glass patterns: interference for widths up to 1.6°, then very little thereafter. The results suggest that for both diagonal and circular patterns, the range of interactions of anti-Glass patterns is about 1.5°, four times the size of the dipole separation.

3.3. Summation

Sensitivity to Glass patterns is known to increase with area (Wilson, Wilkinson, & Asaad, 1997). We therefore asked whether the area of summation may be related to the spatial extent of interaction of Glass and anti-Glass patterns by measuring spatial summation under the conditions of this experiment. Diagonal Glass patterns were curtailed to a diamond, whose sides ran parallel to the orientation of the Glass patterns. Circular Glass patterns were curtailed within a circle of variable diameter.

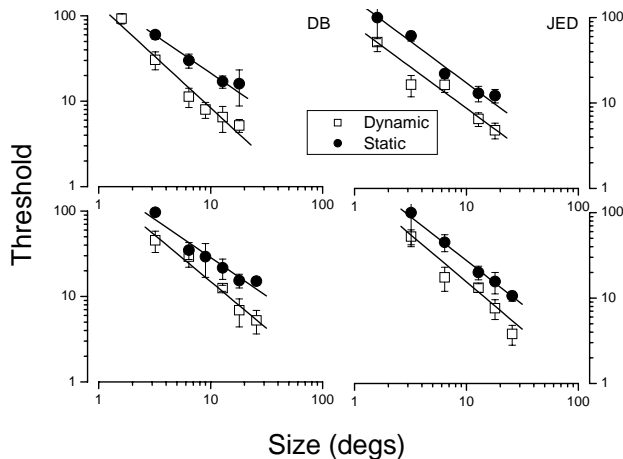


Fig. 6. Dependency of Glass thresholds of stimulus size. The upper curves show results for diagonal translational patterns, lower curves for circular patterns, open square symbols static patterns, filled circles dynamic patterns. The lines passing near the data are best fitting linear regressions (on log–log coordinates). The slopes (for DB and JED, respectively) were: static translational -0.90 , -0.97 ; dynamic translational -1.2 , -0.97 ; static circular -0.90 , -1.00 ; dynamic circular -1.09 , -1.10 . In all cases, thresholds improve over the whole range measured, showing very little sign of asymptote.

The results for both diagonal and circular patterns, static and dynamic stimuli, are shown in Fig. 6. In all conditions, thresholds decreased with stimulus width, with very little sign of saturation over the range measured (20° for diagonal patterns, 30° for circular patterns). The curves are well fit with a linear regression on log–log coordinates (average $r^2 = 0.98$) with slopes nearing unity. This implies a linear dependency of stimulus width, or a square-root dependency of stimulus area, as would be expected from an ideal detector that could attend to the region to which the Glass patterns were confined. These results show that the summation area for Glass patterns was considerably larger than the region of interaction of Glass and anti-Glass stimuli.

4. Discussion

The results reported here show that dipoles of opposite polarity (anti-Glass pattern) hamper the perception of the distinctive pattern of global striation produced by like-polarity dipoles (Glass patterns). However, there is not total cancellation. Thresholds are raised, but detection is still possible.

The lifting of thresholds above levels produced by noise alone occurs over a wide range of densities, and increases with the fourth-root of density. The dependency on density suggests that the interaction between Glass and anti-Glass dipoles is local, not global as a Fourier analysis might suggest (Fig. 1): higher densities leave the structure of the Fourier spectrum untouched but increase the probability of anti-Glass pairs and Glass pairs both falling within some critical local region. What we find when we confine Glass and anti-Glass dipoles into alternating stripes is consistent with a local rather than a global interaction between them.

The size of the effect decreases with strip width up to a width of about 1.6° , and there is no effect thereafter.

On the other hand summation increases with display width well beyond 1.6° . That is to say the interaction among Glass dipoles occurs over a much larger range than the interaction between Glass and anti-Glass dipoles. So too does interaction between Glass dipoles and noise. The proportion of Glass dipoles required for the detection of Glass patterning in noise varied little with density or with stripe width for any of the patterns used in this study. This independence from density and stripe width suggests that the interaction of Glass dipoles with noise occurs not at an early local stage of analysis, as does the interaction of Glass with anti-Glass dipoles, but later and more globally after orientation has been analysed.

The generalizations above apply to all the types of Glass patterns used in this study, translational and circular, each in its standard static and its dynamic version. The thresholds for dynamic patterns are usually lower than those for static patterns (see Figs. 4–6) but otherwise the results for the stimulus types differ little. This is somewhat surprising given the evidence for the existence of mechanisms specialized for the processing of circular Glass patterns but not for similar mechanisms for translational Glass patterns (Wilson & Wilkinson, 1998; but see Dakin & Bex, 2002).

The existence of two stages of analysis of glass patterns finds support in previous studies. For example, Dakin and Bex (2001) created glass patterns from narrow band Laplacian-of-Gaussians, and showed that whereas the individual pairs needed to be of similar spatial frequency to form salient glass patterns (implying local tuning from spatial frequency), random pairs of very different spatial frequency to the dipole elements were very effective masks of coherence (implying pooling of spatial frequencies at the global level). On the other hand, Badcock et al. (2005) showed that pairs of black dots do not sum with pairs of white pairs, or with “textured” (luminance-balanced) dots, suggesting that there is no pooling across ON and OFF channels. This result is surprising, and merits further investigation.

The neural substrate for the first-stage of glass pattern analysis is likely to be V1, where cells with small receptive fields respond to glass patterns in the way that may be expected from their tuning curves (Smith, Bair, & Movshon, 2002). V4 has been suggested as the substrate for the global form perception (Wilson & Wilkinson, 1998), based on the tuning properties of these cells (Gallant, Braun, & Van Essen, 1993), and their larger receptive field sizes (although possibly not large enough to account for the summation of 40° observed here, tending to be 6° at most: Desimone & Schein, 1987). In humans, imaging studies have shown that areas activated by glass-like coherence patterns include regions in the middle occipital gyrus, the ventral occipital surface, the intraparietal sulcus, and the temporal lobe (Braddick, O’Brien, Wattam-Bell, Atkinson, & Turner, 2000). The exact location of the integration site is still uncertain, but it does seem clear that it occurs at a stage after primary cortex V1.

That thresholds for dynamic patterns are lower than for static patterns can be attributed to signal summation (probabilistic or otherwise) since each dynamic pattern consists of a sequence of independent patterns of the same type. But though their thresholds are lower, dynamic patterns are no more immune from the depredations of anti-Glass than static patterns. This again suggests that anti-Glass dipoles exert their effects at an early stage. Dynamic Glass patterns appear to stream coherently and the streaming could reveal the presence of Glass patterning that was otherwise undetectable. That appearance of streaming confers no protection from anti-Glass dipoles suggests that they do their damage early.

Acknowledgments

We acknowledge support from the Australian ARC and NHMRC, and Italian ministry for Universities and Research.

References

- Badcock, D. R., Clifford, C. W., & Khuu, S. K. (2005). Interactions between luminance and contrast signals in global form detection. *Vision Research*, 45(7), 881–889.
- Barlow, H. B., & Olshausen, B. A. (2004). Convergent evidence for the visual analysis of optic flow through anisotropic attenuation of high spatial frequencies. *Journal of Vision*, 4(6), 415–426.
- Braddick, O. J., O'Brien, J. M., Wattam-Bell, J., Atkinson, J., & Turner, R. (2000). Form and motion coherence activate independent, but not dorsal/ventral segregated, networks in the human brain. *Current Biology*, 10(12), 731–734.
- Dakin, S. C. (1997). The detection of structure in glass patterns: Psychophysics and computational models. *Vision Research*, 37(16), 2227–2246.
- Dakin, S. C., & Bex, P. J. (2001). Local and global visual grouping: Tuning for spatial frequency and contrast. *Journal of Vision*, 1(2), 99–111.
- Dakin, S. C., & Bex, P. J. (2002). Summation of concentric orientation structure: Seeing the Glass or the window? *Vision Research*, 42(16), 2013–2020.
- Desimone, R., & Schein, S. J. (1987). Visual properties of neurons in area V4 of the macaque: Sensitivity to stimulus form. *Journal of Neurophysiology*, 57(3), 835–868.
- Efron, B., & Tibshirani, R. J. (1993). An introduction to the bootstrap. In *Monographs on statistics and applied probability*, 57, New York: Chapman & Hall.
- Gallant, J. L., Braun, J., & Van Essen, D. C. (1993). Selectivity for polar, hyperbolic, and Cartesian gratings in macaque visual cortex. *Science*, 259(5091), 100–103.
- Glass, L. (1969). Moiré effects from random dots. *Nature*, 223, 578–580.
- Glass, L., & Perez, R. (1973). Perception of random dot interference patterns. *Nature*, 246(5432), 360–362.
- Glass, L., & Switkes, E. (1976). Pattern recognition in humans: Correlations which cannot be perceived. *Perception*, 5(1), 67–72.
- Kovacs, I., & Julesz, B. (1992). Depth, motion, and static-flow perception at metaisoluminant color contrast. *Proceeding of the National Academy of Science of the United States of America*, 89(21), 10390–10394.
- Prazdny, K. (1986). Some new phenomena in the perception of glass patterns. *Biological Cybernetics*, 53(3), 153–158.
- Ross, J., Badcock, D. R., & Hayes, A. (2000). Coherent global motion in the absence of coherent velocity signals. *Current Biology*, 10, 679–682.
- Smith, M. A., Bair, W., & Movshon, J. A. (2002). Signals in macaque striate cortical neurons that support the perception of glass patterns. *Journal of Neuroscience*, 22(18), 8334–8345.
- Watson, A. B., & Pelli, D. G. (1983). QUEST: A Bayesian adaptive psychometric method. *Perception & Psychophysics*, 33(2), 113–120.
- Wilson, H. R., & Wilkinson, F. (1998). Detection of global structure in Glass patterns: Implications for form vision. *Vision Research*, 38(19), 2933–2947.
- Wilson, H. R., Wilkinson, F., & Asaad, W. (1997). Concentric orientation summation in human form vision. *Vision Research*, 37, 2325–2330.
- Wilson, J. A., Switkes, E., & De Valois, R. L. (2004). Glass pattern studies of local and global processing of contrast variations. *Vision Research*, 44(22), 2629–2641.